Resistance forces on an intruder penetrating partially fluidized granular media

Chuan-Ping Liu,* Shuo Bai, and Li Wang
School of Energy and Environmental Engineering, University of Science and Technology Beijing, Beijing 10083, China

(Received 7 July 2018; published 15 January 2019)

This paper analyzes the forces on a cylindrical straight rod penetrated into a granular bed in the partially fluidized state. As gas flow is blown from the bed bottom, the resistance force decreases linearly with increasing gas flow velocity. After the bed is fluidized, the resistance force is close to zero. When the bed is under the action of vibration, the average resistance force ($F_{b,\mathrm{ave}}$) linearly decreases with increasing vibration acceleration but is barely influenced by the vibration frequency. The bed cannot be completely liquefied under vibration only, and $F_{b,\mathrm{ave}}$ constantly exists with increasing vibration acceleration. Based on the equivalent effects of gas flow and vibration, the calculation formula of the resistance force in the partially fluidized bed is established as $F_{b,\mathrm{ave}}/F_{b,0} = 1-u/u_{\mathrm{MF}}-0.748\Gamma$, and the minimum vibration liquid velocity is estimated as $u_{\mathrm{ML}}/u_{\mathrm{MF}} = 1-0.748\Gamma$.

DOI: 10.1103/PhysRevE.99.012903

I. INTRODUCTION

Granular materials comprise a large discrete system featuring particle sizes greater than 1 μm. Molecular forces can be ignored and Brownian motion is absent in the granular system scale. Classical mechanics can provide an exact solution of the motion of each particle, and a system composed of a large number of particles shows interesting static and dynamic characteristics [1–4]. A common method used to estimate the characteristics of granular materials is measurement of the forces on an intruder immersed in a granular layer.

Strong forces act on an immersed object moving in a statically packed granular bed. The horizontal dragging or stirring force [5–7] on the immersed object is proportional to its cross-sectional area but is barely influenced by the moving speed. Stone *et al.* [8,9] pushed a flat plate vertically through a dense granular medium and found that the resistance exerted on the flat plate increases linearly with increasing immersion depth in the upper region of the bed. Albert *et al.* [7] vertically inserted a rod into a granular bed and rotated the granular bed to reveal that the torsion on the rod is proportional to the square of the immersion depth.

The force chains among granules are weakened and forces on the immersed object decrease when gas flow is blown into the granular layer. Brzinski III and Durian [10] blew gas from the bed bottom and measured the rotational torque of an immersed T bar; their results showed that the torque linearly decreases with increasing gas flow velocity. When the gas flow velocity is greater than a certain critical velocity, the granular bed shows a liquidlike characteristic, i.e., fluidization. This critical velocity is called the minimum fluidized velocity u_{MF}. Measurement of u_{MF} mostly follows the "pressure drop–gas flow velocity" curve method [11–13]. The gas flow velocity increases until the pressure drop of the bed is equal to its gravity, and the corresponding velocity is considered the minimum fluidized velocity u_{MF}.

Vibration can fluidize a granular bed and affect the forces exerted on an immersed object. The force on an immersed object is proportional to its volume and increases with increasing vibration acceleration under the horizontal vibration of the granular bed [14,15]. Liu *et al.* [16] vertically vibrated a bed and found that the force on the immersed object is greater than the Archimedean buoyancy and varies nonlinearly with the change in depth before the bed is fluidized. Zhou *et al.* [13] discussed the minimum fluidized velocity of a vibration fluidized bed u_{MV} based on the computation method of u_{MF}. Introduction of vibration can reduce u_{MV}, and vibration can replace the effects of gas flow during bed fluidization to some extent.

Existing studies have mostly focused on the force exerted on immersed objects in a statically packed granular [5–9] or completely fluidized [11–13] bed. Occasionally, the vibration strength and gas velocity are too weak to fluidize the granular layer completely, such as during vibration transport or fixed bed drying. In this paper, this granular layer state is defined as a partially fluidized state. The gas velocity in a partially fluidized bed is notably smaller than the minimum fluidized velocity.

Given the strong interaction between gas flow and vibration, partially fluidized beds show characteristics different from those of statically packed and completely fluidized beds. To investigate the properties of the granular layer in a partially fluidized bed and clarify the equivalent effects of gas flow and vibration, this paper penetrates straight rods into a partially fluidized bed and analyzes the forces acting on these rods.

II. EXPERIMENTAL SETUP

A schematic of the experimental setup is shown in Fig. 1. A plexiglass cylindrical bed with an internal diameter (D) of 180 mm is used in all the experiments, and experimental particles are filled into the bed to form a 190-mm-high (H) granular bed. The experimental particles are spherical corundum beads with an average diameter (d_s) of 0.75 mm, size distribution of 0.5–1 mm, material density (ρ_s) of 4303 kg/m^3, bulk density

*Corresponding author: cpliu@ustb.edu.cn

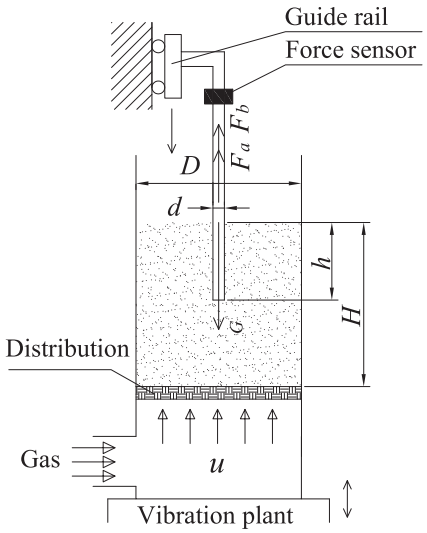

FIG. 1. Sketch of the experimental setup. The granular bed is set on a vibration plant, and gas is blown from the distribution at the bed bottom. A cylinder rod is penetrated into the granular bed, and the resistance forces are measured and discussed.

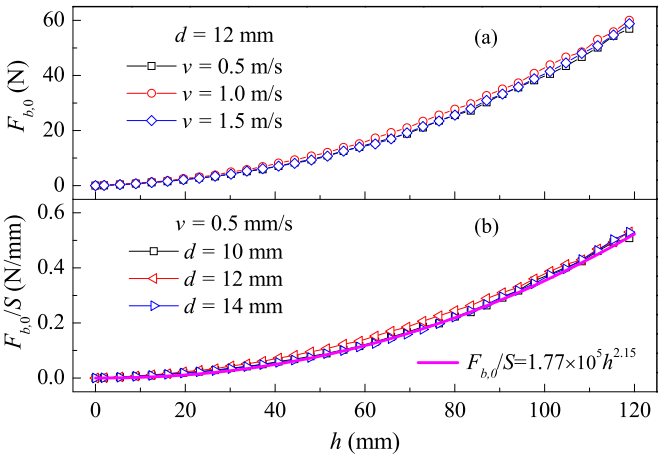

FIG. 2. Resistance forces on a rod penetrating into a statically packed granular bed at $u = 0$. (a) Different penetration speeds of the 12-mm-diameter rod. The resistance force is independent of the penetration speed. (b) Different rod sizes with the same resistance velocity, $v = 0.5$ m/s. The resistance force is proportional to the area of the rod section.

(ρ_φ) of 2286 kg/m^3, and minimum fluidization velocity (u_{MF}) of 0.65 m/s.

The gas is obtained from a gas fan and blown into the granular bed through a gas chamber. A porous gas distributor is installed at the bottom of the bed to enable uniform gas flow into the granular bed. The gas flow velocity (u) in the bed is calculated by measuring the gas flux and controlled using a frequency conversion fan in our experiments. In our experiments, the range of gas flow velocities is 0−0.72 m/s, i.e., $0 \leqslant u/u_{\mathrm{MF}} \leqslant 1.12$. The bed and gas chamber are fixed on an electromagnetic shaker (LDS V555). Therefore, the vibration of the granular bed is controlled by changing the vibration amplitude and frequency of the shaker. The shaker is vertically vibrated following the protocol $z(t) = A\sin(2\pi f t)$, where z is the vertical coordinate of the shaker plate, t is the vibration time, and A and f are the vibration amplitude and frequency, respectively. In accordance with the shaker vibration protocol, the vibration acceleration (a) is expressed as $a = A(2\pi f)^2$.

The length of the stainless-steel rods used in the experiments is 250 mm, and their diameters (d) are 10, 12, and 14 mm. Each rod is vertically penetrated into the bed center, and the distance from the rod bottom to the bed surface is defined as the penetration depth (h). The rod is fixed to the vertical electric rail through a force sensor. Pushing and pulling of the rod are controlled by the movement of the rail, and the penetration force is measured by using a force sensor.

An Agilent recorder (model 34972A) is used to record the force values on the moving rod with a recording frequency of 1080 Hz. The resulting data are expressed as the average of every 3600 recorded values (2 s). The reading value of the force sensor is expressed as F_m. During force balance analysis of the rod, the penetration force exerted on the rod by the granular bed is obtained as $F = F_m - G$, where G is the gravity of the rod. F can be mainly divided into two parts, i.e., $F = F_a + F_b$, where F_a is the Archimedes force and F_b is the resistance force caused by the force chains in the granular bed, where $F_a = \rho_\varphi g S h$, S is the cross-sectional area of the rod, and $S = \pi d^2/4$. The Archimedes force (F_a) is proportional to the penetration depth, and the resistance force (F_b) is discussed in detail below.

III. RESULTS AND DISCUSSION

A. Statically packed bed

A rod of $d = 12$ mm is penetrated into the statically packed granular bed at different penetration speeds ($v = 0.5$, 1.0, and 1.5 mm/s), and the corresponding resistance forces are shown in Fig. 2(a); here, $F_{b,0}$ is the resistance force in the statically packed bed. During rod penetration, the resistance force on the rod superlinearly increases with increasing immersion depth. Under different penetration speeds, $F_{b,0}$ is approximately identical under the same immersion depth, i.e., the force on the rod is independent of its penetration speed.

Rods with different diameters ($d = 10$, 12, and 14 mm) are penetrated into the bed from the surface at a velocity of 0.5 mm/s. The resistance forces are shown in Fig. 2(b), where S is the cross-sectional area of the rod. The scale of the resistance force with penetration depth ($F_{b,0}/S$) remains nearly identical under different penetration speeds and different rod sizes. The resistance force is linear to the cross-sectional areas and increases with increasing penetration depth. Here, the force on the rod is fitted by using a power-law function as $F_{b,0}/S = kh^n$, where $k = 1.77 \times 10^{-5}$ and $n = 2.15$ under our experimental conditions.

B. Bottom blowing bed

Gas flow is blown into the granular bed, and a rod of $d = 12$ mm is penetrated into the bed at a speed of $v = 1$ mm/s . Figure 3(a) shows the resistance forces F_b on the rod along the penetration depth with changes in gas velocity; in the figure, the solid line is the Archimedean force $F_a(F_a = \rho_\varphi g S h)$.

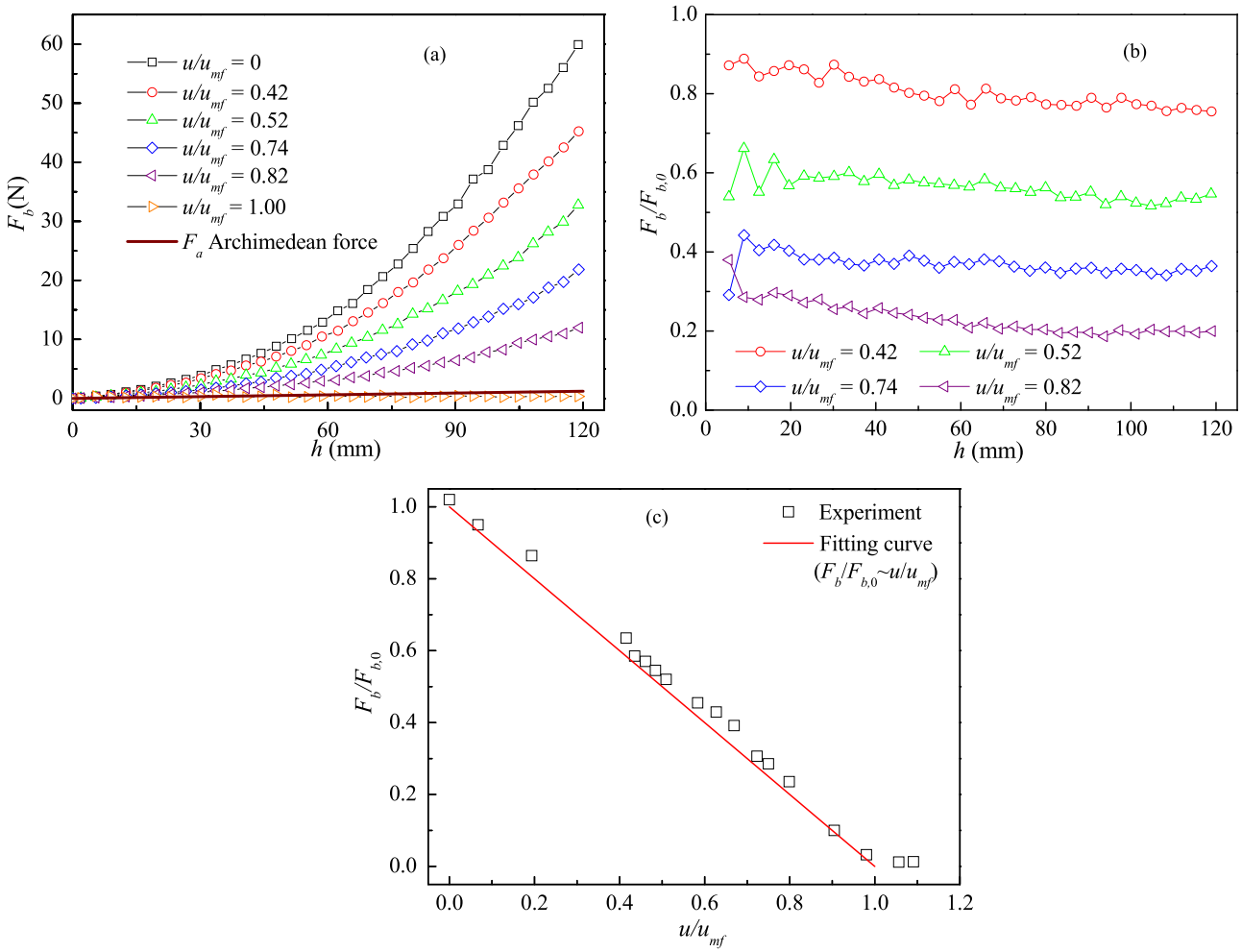

FIG. 3. Resistance force on the rod penetrated in the bottom blowing bed. (a) Changes in resistance force with the penetration depth. The force decreases with increasing gas flow velocity. (b) Changes in dimensionless force with the penetration depth. $F_b/F_{b,0}$ slightly changes at a fixed gas flow velocity. (c) Relationship between resistance force and gas velocity. $F_b/F_{b,0}$ shows a linear relationship with u/u_{MF}.

F_b is positive and usually far larger than F_a in a statically packed or partially fluidized bed. F_b is approximately close to zero when the bed is completely fluidized ($u/u_{\mathrm{MF}} = 1$). Blowing of gas flow can reduce the resistance force F_b, and F_b decreases with increasing gas flow velocity. The dimensionless resistance force is defined as $F_b/F_{b,0}$. Figure 3(b) presents $F_b/F_{b,0}$ at different penetration depths. The changes in $F_b/F_{b,0}$ are minor under a fixed u/u_{MF}.

Figure 3(c) reveals the relationship between $F_b/F_{b,0}$ and u/u_{MF}, where $F_b/F_{b,0}$ is the average value from $h = 0$ to 120 mm at the corresponding u/u_{MF}. When $u/u_{\mathrm{MF}} < 1$, $F_b/F_{b,0}$ linearly decreases with increasing u/u_{MF}. When $u/u_{\mathrm{MF}} > 1$, $F_b/F_{b,0}$ remains constant and is close to zero with changes in u/u_{MF}. As shown in the fitting curve of Fig. 3(c), $(F_b/F_{b,0}) = U^*$ when $u/u_{\mathrm{MF}} < 1$, where $U^* = (1-u/u_{\mathrm{MF}})$. This result (the relationship between resistance force and gas velocity) is consistent with the function of the T-bar rotation torque and gas velocity in the experiments of Brzinski III and Durian [10].

As the rod penetrates the statically packed bed, the particles in the rod front are pushed away. The rod imposes a strong pushing force F_p (counterforce of F_b, $F_p = F_b$) on the front particles, and F_p is transmitted and dispersed forward via the force chains of the granular media. During transmission, F_p is dispersed, and the directions of the component forces change. Most of the component forces act on the bed bottom and bed wall, and only the upward component force $F_{p,\mathrm{up}}$ presses on the upper granular layer. The particles around the rod move upward, and a space is formed for rod penetration when the upward force overcomes the pressure of the upper granular layer G_{layer}($G_{\mathrm{layer}} \geqslant F_{p,\mathrm{up}} = \beta F_b$, where β is the ratio between $F_{p,\mathrm{up}}$ and F_p).

The pressure of the upper granular layer is influenced by the penetration depth of the rod. The deeper a rod is immersed, the stronger the pressure exerted on it. Larger immersion depths cause larger resistance forces F_b, as shown in Fig. 2.

Gas flow can also affect the force chains. The upward drag force of a gas flow applied to the granular bed acts against G_{layer}. The upward drag force can decrease G_{layer} when the gas velocity is less than the minimum fluidization velocity ($u/u_{\mathrm{MF}} < 1$). A large gas velocity corresponds to a small equivalent gravitational acceleration (g_{eff}), where $g_{\mathrm{eff}} = g(1-u/u_{\mathrm{MF}})$. The pressure of the upper granular layer is induced by the difference between the layer gravity and the

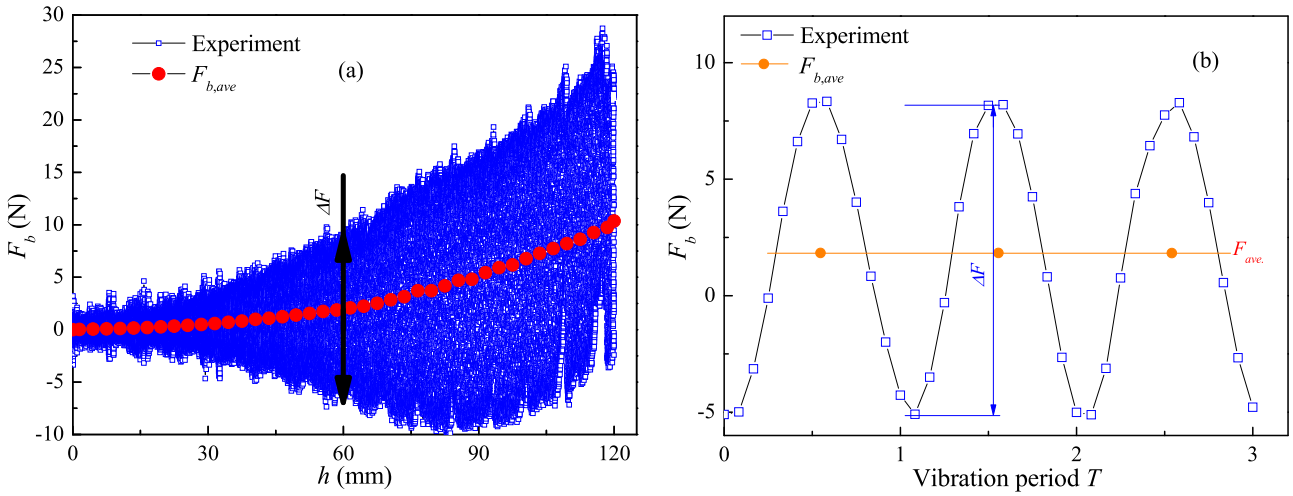

FIG. 4. Resistance forces on a rod penetrating into a vibration bed at $u = 0$. (a) $f = 90\,\mathrm{Hz}$ and $a = 9.8\,\mathrm{m/s^2}$. The resistance force fluctuates during penetration. With increasing penetration depth, both the force and the force fluctuation increase. The rod dots present the average forces at each penetration depth. (b) Force fluctuation at a penetration depth of $h = 60\,\mathrm{mm}$.

upward drag force, $G_{\mathrm{layer}} \propto g_{\mathrm{eff}} = g(1-u/u_{\mathrm{MF}})$. Therefore, $F_b \propto 1-u/u_{\mathrm{MF}}$ and $F_b/F_{b,0} = U^*$, as shown in Fig. 3(c).

When the granular bed is completely fluidized ($u/u_{\mathrm{MF}} \geqslant 1$), the upward drag force of the gas flow is equal to $G_{\mathrm{layer}}(g_{\mathrm{eff}} = 0)$. Under this condition, the resistance force is approximately equal to zero ($F_b = 0$), i.e., the penetration force on the rod is approximately equal to the Archimedean buoyancy ($F = F_a$). The granular bed exhibits a liquidlike characteristic, and the gas flow completely fluidizes the granular bed.

C. Vibration bed

The granular bed is vibrated at a frequency $f = 90\,\mathrm{Hz}$ and the vibration acceleration is $a = 9.8\,\mathrm{m/s^2}$. In the vibration bed, no gas flow is blown from the bed bottom, and $u = 0$. A rod with $d = 12\,\mathrm{mm}$ is penetrated into the vibration bed. Figure 4(a) shows the resistance forces F_b acting on the rod when the recording frequency of the Agilent recorder is 1080 Hz.

In the case of vibration, F_b remarkably fluctuates during penetration. Figure 4(b) shows F_b under three bed vibration periods at $h = 60\,\mathrm{mm}$. The period of the force is notably identical to the vibration period of the bed. Force fluctuation is defined as the difference between the maximum and minimum forces at a certain penetration depth of the rod, $\Delta F = (F_{b,\max} - F_{b,\min})$, and the average resistance force $F_{b,\mathrm{ave}}$ is defined as the mean value of F_b on the rod during the vibration period. For the vibration bed, $F_{b,\mathrm{ave}}$ superlinearly increases, and ΔF first rapidly increases and then slowly increases with increasing penetration depth of the rod.

Figure 5(a) shows the average resistance force $F_{b,\mathrm{ave}}$ on a rod penetrating into a vibration bed with changing vibration acceleration; in this case, the vibration frequency is fixed to $f = 90\,\mathrm{Hz}$ and the vibration amplitude is varied to achieve accelerations of a. The solid line in Fig. 5(a) is the Archimedean force F_a. Introduction of vibration can decrease the resistance force $F_{b,\mathrm{ave}}$, and $F_{b,\mathrm{ave}}$ monotonously decreases with increasing vibration acceleration. In fact, most of the resistance forces acting on the rod come from the bed bottom and bed wall due to the bed arches and force chains. Destruction of the bed arches and force chains is strengthened with increasing vibration acceleration [18]. Therefore, the resistance force on the rod decreases with increasing vibration acceleration.

In the absence of vibration ($a = 0$), the resistance force F_b is relatively stable, and the force fluctuation ΔF is approximately equal to zero. Force fluctuations occur during bed vibration. Figure 5(b) shows the force fluctuation with changes in vibration acceleration. When $a < 9.8\,\mathrm{m/s^2}$, ΔF increases with increasing vibration acceleration. The ΔF–h curve is convex, and ΔF gradually increases to a certain maximum value and remains constant with further increases in the penetration depth of the rod. When $a > 9.8\,\mathrm{m/s^2}$, the ΔF–h curve is gradually converted from convex to concave with increasing vibration acceleration.

Figure 6 shows the average resistance force $F_{b,\mathrm{ave}}$ on a rod penetrating into a vibration bed with changing vibration frequency ($f = 70$, 90, and 100 Hz). The vibration frequency slightly affects the average resistance force and force fluctuation.

The interaction between the granular layer and bed bottom differs under different vibration accelerations. The granular layer consistently moves up and down synchronously with the bed when the vibration acceleration is smaller than $9.8\,\mathrm{m/s^2}$, and the particles remain relatively still at the bed bottom. The force fluctuations at the bottom layers are similar, and the changes in ΔF are small. When the vibration acceleration exceeds $9.8\,\mathrm{m/s^2}$, the granular layer is thrown out of the bed bottom. The particles move up and collide with each other, and the vibration energy (kinetic energy) is dissipated during transferring from the bottom to the top of the bed. Therefore, force fluctuations increase with the bed depth. In other words, different variations of ΔF with bed depth are induced by the fluidization state. When the bed is in a partially fluidized state, ΔF gradually increases to a certain maximum value and then remains constant with increasing h. Obviously, bed

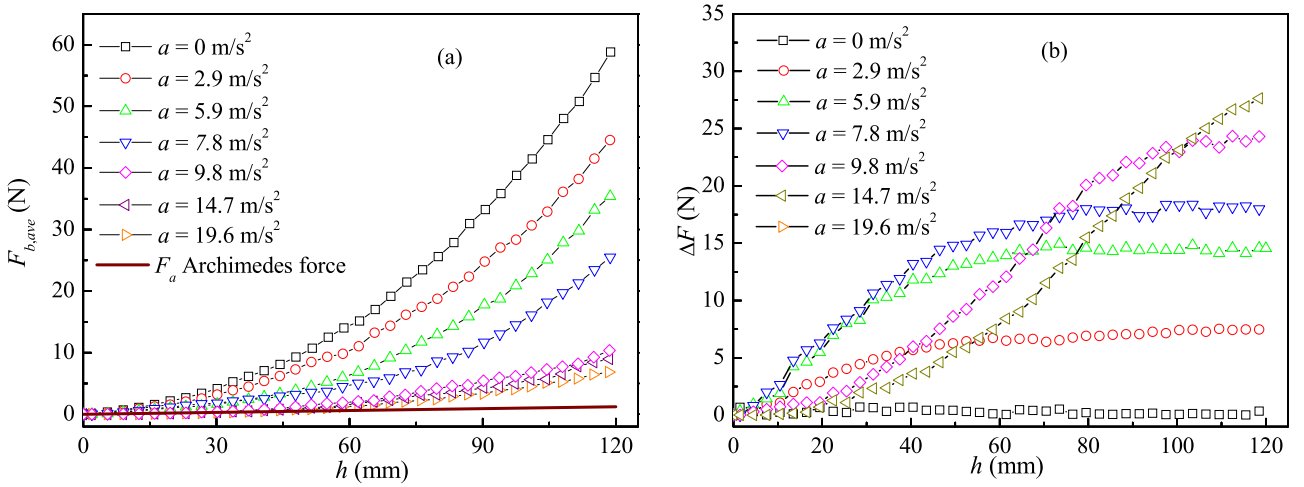

FIG. 5. Effect of vibration acceleration on the resistance force at $u = 0$ and $f = 90$ Hz. (a) The resistance force decreases with increasing vibration acceleration. (b) The force fluctuation ΔF at different vibration accelerations. ΔF exhibits a convex function related to the penetration depth when the vibration acceleration is smaller than 9.8 m/s^2 and an S function when the vibration acceleration is larger than 9.8 m/s^2.

fluidization is not only dependent on vibration parameters but also related to the gas flow velocity. The equivalent effects of gas flow and vibration are discussed in Sec. III D.

Figure 7 shows the relationship between the dimensionless average resistance force $F_{b,\mathrm{ave}}/F_{b,0}$ and the dimensionless strength $\Gamma(\Gamma = a/g)$ with changing vibration parameters. The resistance force on the rod remains relatively constant with changes in vibration frequency. As the vibration strength increases, $F_{b,\mathrm{ave}}/F_{b,0}$ decreases linearly and then remains constant. A critical vibration strength (Γ_c) that is slightly greater than 1 exists. $F_{b,\mathrm{ave}}/F_{b,0} = \Gamma^*$ when the vibration strength is less than Γ_c, where $\Gamma^* = (1-0.748\Gamma)$. When the vibration strength is greater than Γ_c, the vibrations slightly affect $F_{b,\mathrm{ave}}/F_{b,0}$.

Figure 3 shows that the granular bed can be completely fluidized when gas flow is blown from the bed bottom and exhibits a liquidlike characteristic. When the bed is vibrated, the particles collide with one another, and the internal force chains in the bed are destroyed. The fluidity of the bed is improved. Vibration shows effects similar to those of gas flow, which enables the granular bed to exhibit a liquidlike characteristic, as shown in Fig. 7.

D. Gas vibration bed

Here, the granular bed that is simultaneously vibrated and experiences gas flow from the bed bottom is called the gas vibration bed, and the combined factor is defined as $U^* + \Gamma^* - 1$. The average resistance force varies when the rod is penetrated into the gas vibration bed by changing the gas velocity or vibration strength. Figure 8 shows the relationship between the dimensionless average resistance force $F_{b,\mathrm{ave}}/F_{b,0}$ and the combined factor $U^* + \Gamma^* - 1$. The results show that a relationship of $F_{b,\mathrm{ave}}/F_{b,0} = U^* + \Gamma^* - 1$ exists when $U^* + \Gamma^* - 1 > 0$, $0 < U^* < 1$ (i.e., $u/u_{\mathrm{MF}} < 1$), and $0.252 < \Gamma^* < 1$ (i.e., $\Gamma < 1$).

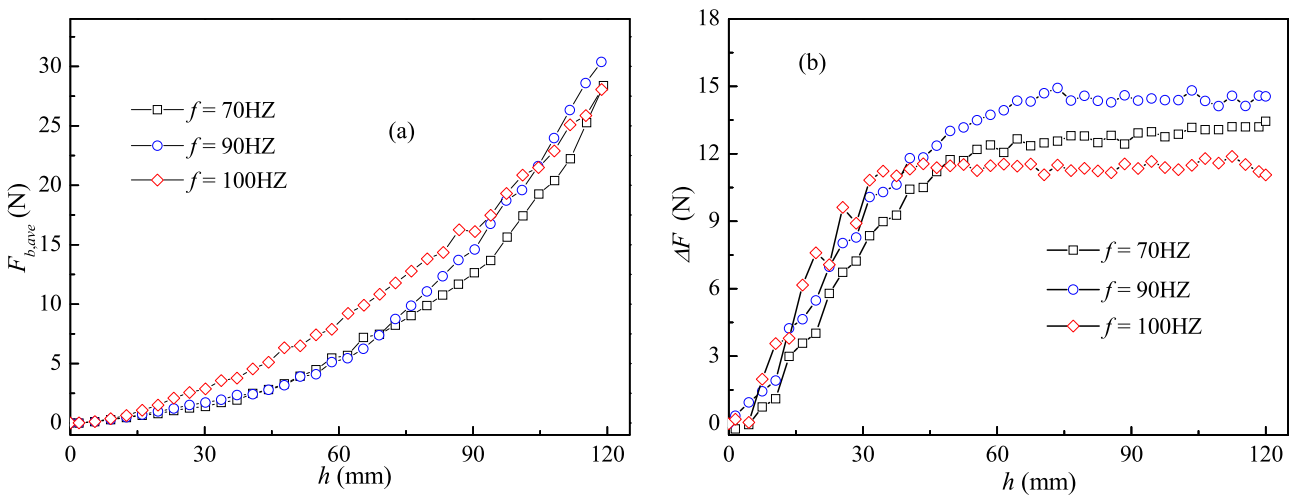

FIG. 6. Effect of vibration frequency on the resistance force at $u = 0$ and $a = 5.8$ m/s^2. As the vibration frequency changes ($f = 70$, 90, and 100 Hz), both the resistance force (a) and the force fluctuation (b) barely vary under a fixed vibration acceleration.

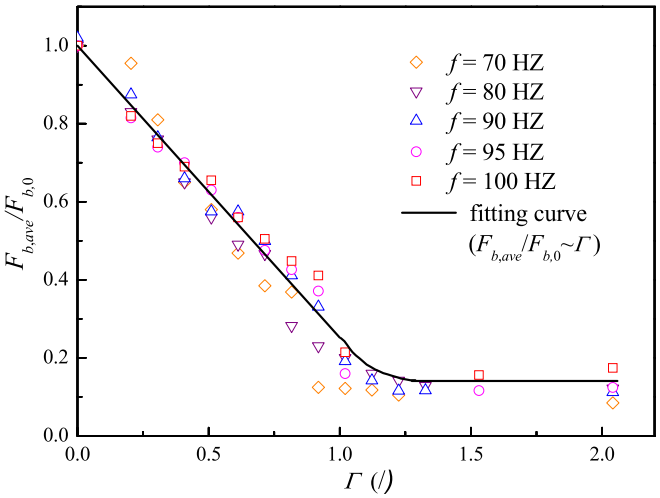

FIG. 7. Relationship between the dimensionless force and dimensionless vibration strength at $u = 0$. The dimensionless average resistance force $F_{b,\mathrm{ave}}/F_{b,0}$ shows a linear relationship with the dimensionless vibration strength Γ when $\Gamma < 1.1$.

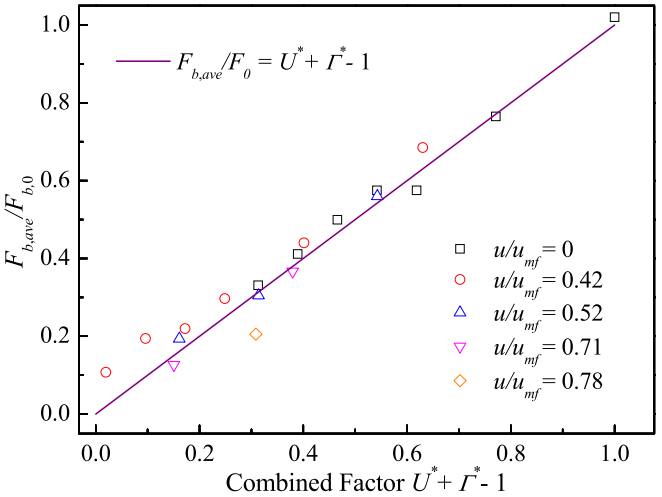

FIG. 8. Relationship between $F_{b,\mathrm{ave}}/F_{b,0}$ and the combined factor $U^* + \Gamma^* - 1$. The dimensionless average resistance force is approximately equal to the combined factor.

In previous studies [11–13,17–20], the minimum fluidization velocity of the vibration bed (u_{MV}) was determined by using the pressure drop–gas flow velocity curve method. As shown in Table I, the minimum fluidization velocity decreases with increasing vibration parameters. Considering the resistance force, the bed possesses a liquid property, i.e., the bed is liquefied when $F_b = 0$ or $F_{b,\mathrm{ave}} = 0 (F = F_a)$, and the corresponding gas flow velocity is defined as the minimum vibration liquid velocity u_{ML}. From $U^* + \Gamma^* - 1 = 0$, we can conclude that $u_{\mathrm{ML}}/u_{\mathrm{MF}} = 1 - 0.748\Gamma$.

The u_{ML} obtained in the present paper shows similar expression with the u_{MV} obtained by Mushtaev *et al.* [17] and Pakowski *et al.* [18] ($u_{\mathrm{MV}}/u_{\mathrm{MF}}$ shows a linear function with Γ, as shown in Table I). By comparison, the yield stress is weakened before the bed is fluidized, and the minimum vibration liquid velocity u_{ML} is smaller than that of the vibration fluidized velocity u_{MV} under the same condition.

IV. CONCLUSION

The resistance force exerted on a rod vertically penetrating into a granular bed is independent of the penetration speed, proportional to the cross-sectional area of the rod, and related to the penetration depth by a 2.15-order power law. When gas flow is blown from the bed bottom, the resistance force decreases linearly with increasing gas flow velocity and decreases to zero when the bed is fluidized.

When the bed is vibrated, the resistance force on the rod is barely influenced by the frequency of vibration. The vibration acceleration is a critical parameter influencing the vibration bed, and the force decreases with increasing vibration acceleration. The dimensionless force ($F_{b,\mathrm{ave}}/F_{b,0}$) decreases linearly with increasing vibration strength and is expressed as $F_{b,\mathrm{ave}}/F_{b,0} = 1 - 0.748\Gamma$. $F_{b,\mathrm{ave}}$ cannot decrease to zero under vibration only. When $\Gamma > 1$, the resistance force remains relatively constant and no longer changes with changes in Γ.

Vibration and gas flow exert equivalent effects on the forces of the penetrated object. When vibration and flow blowing are applied to the granular bed simultaneously, the resistance force can be expressed as $F_{b,\mathrm{ave}}/F_{b,0} = U^* + \Gamma^* - 1$, where $U^* = 1 - u/u_{\mathrm{MF}}$ and $\Gamma^* = 1 - 0.748\Gamma$. From the equivalent effects of the force on the plugging object, the minimum vibrated liquid velocity can be obtained as $u_{\mathrm{ML}}/u_{\mathrm{MF}} = 1 - 0.748\Gamma$, which has similar expression with the minimum vibration fluidized velocity but is much smaller.

ACKNOWLEDGMENTS

The authors are grateful for the support of the National key research and development plan of China (No. 2016YFB0601101) and the National Natural Science Foundation of China (Grant No. 51506006).

TABLE I. u_{MV} of the vibrated fluidized bed based on the pressure drop–gas flow velocity curve [17–20].

	Expression
Rahul and Mujumdar [19]	$u_{\mathrm{MV}}/u_{\mathrm{MF}} = 1.952 - 0.275 - 0.686\Gamma^2$
Mushtaev *et al.* [17]	$u_{\mathrm{MV}} = 0.12(\rho_p/\rho_g)^{0.63}(\rho_p/\mu)^{0.63} {d_p}^{0.88}(1 - 0.095\Gamma)$
Pakowski *et al.* [18]	$u_{\mathrm{MV}}/u_{\mathrm{MF}} = 1 - 0.09\Gamma$
Jin [20]	$u_{\mathrm{MV}}/u_{\mathrm{MF}} = 1 - 0.41[{d_p}^3\rho_g(\rho_s - \rho_g)g/\mu^2]^{-0.167}(H_0/A)\Gamma^{0.64}$

[1] H. M. Jaeger, S. R. Nagel, and R. P. Behringer, Granular solids, liquids, and gases, Rev. Mod. Phys. **68**, 1259 (1996).

[2] M. E. Möbius, B. E. Lauderdale, S. R. Nagel, and H. M. Jaeger, Size separation of granular particles, Nature (London) **414**, 270 (2001).

[3] V. Trappe, V. Prasad, L. Cipelletti, P. N. Segre, and D. A. Weitz, Jamming phase diagram for attractive particles, Nature (London) **411**, 772 (2001).

[4] E. E. Ehrichs, H. M. Jaeger, G. S. Karczmar, J. B. Knight, V. Y. Kuperman, and S. R. Nagel, Granular convection observed by magnetic resonance imaging, Science **267**, 1632 (1995).

[5] R. Candelier and O. Dauchot, Creep Motion of an Intruder Within a Granular Glass Close to Jamming, Phys. Rev. Lett. **103**, 128001 (2009).

[6] D. J. Costantino, J. Bartell, K. Scheidler, and P. Schiffer, Low-velocity granular drag in reduced gravity, Phys. Rev. E **83**, 011305 (2011).

[7] R. Albert, M. A. Pfeifer, A.-L. Barabási, and P. Schiffer, Slow Drag in a Granular Medium, Phys. Rev. Lett. **82**, 205 (1999).

[8] M. B. Stone, D. P. Bernstein, R. Barry, M. D. Pelc, Y. K. Tsui, and P. Schiffer, Getting to the bottom of granular medium, Nature (London) **427**, 503 (2004).

[9] M. B. Stone, R. Barry, D. P. Bernstein, M. D. Pelc, Y. K. Tsui, and P. Schiffer, Local jamming via penetration of a granular medium, Phys. Rev. E **70**, 041301 (2004).

[10] T. A. Brzinski III and D. J. Durian, Characterization of the drag force in a gas-moderated granular bed, Soft Matter **6**, 3038 (2010).

[11] J. F. Richardson, *Incipient Fluidization and Particulate Systems*, in *Fluidization*, edited by J. F. Davidson and D. Harrison (Academic, New York, 1971), Chap. 2, p. 25.

[12] S. B. Maiti, S. Let, N. Bar, and S. K. Das, Non-spherical solid-non-Newtonian liquid fluidized and ANN modelling: Minimum fluidization velocity, Chem. Eng. Sci. **176**, 233 (2018).

[13] E. Zhou, Y. Zhang, Y. Zhao, Z. Luo, J. He, and C. Duan, Characteristic gas velocity and fluidization quality evaluation of vibrated dense medium fluidized bed for fine coal separation, Adv. Powder Technol. **29**, 985 (2018).

[14] D. A. Huerta, Victor Sosa, M. C. Vargas, and J. C. Ruiz-Suárez, Archimedes' principle in fluidized granular systems, Phys. Rev. E **72**, 031307 (2005).

[15] C. Maes and S. R. Thoma, Archimedes' law and its corrections for an active particle in a granular sea, J. Phys. A **44**, 285001 (2011).

[16] C. Liu, F. Zhang, L. Wang, and S. Zhan, An investigation of forces on intruder in a granular material under vertical vibration, Powder Technology **247**, 14 (2013).

[17] V. I. Mushtaev, B. M. Korotkov, and V. A. Chevilenko, Hydrodynamic phenomena during the drying of polymer materials in a vibrating fluidized bed, Chem. Pet. Eng. **9**, 1083 (1973).

[18] Z. Pakowski, A. S. Mujundar, and C. Strumillo, Theory and application of vibrated beds and vibrated fluid beds for drying processes, Adv. Drying **3**, 245 (1993).

[19] G. Rahul and A. S. Mujumdar, Aerodynamics of a vibrated fluid bed, Can. J. Chem. Eng. **58**, 332 (1980).

[20] H. Jin, *Fluidization Characteristics and Particle Separation in Vibrated Fluidized Beds* (Institute of Coal Chemistry, Chinese Academy of Sciences, Taiyuan, 1998).